Science of the Total Environment 905 (2023) 167327

Contents lists available at ScienceDirect

Science of the Total Environment

journal homepage: www.elsevier.com/locate/scitotenv

Modelling greenhouse gas emissions from biological wastewater treatment by GPS-X: The full-scale case study of Corleone (Italy)

Hazal Gulhan [a,b], Alida Cosenza [a,*], Giorgio Mannina [a]

[a] Engineering Department, Palermo University, Viale delle Scienze, Build. 8, 90128 Palermo, Italy
[b] Environmental Engineering Department, Civil Engineering Faculty, Istanbul Technical University, Ayazaga Campus, Maslak, 34469 Istanbul, Turkey

HIGHLIGHTS

- A new ASM1 + N_2O mathematical model was proposed and applied to a full-scale WWTP.
- Mathematical model was calibrated and validated by using extensive data.
- The model application was performed to optimise plant operation.
- Scenario analysis on dissolved oxygen and sludge recirculation (RAS) ratio done.
- Best operation scenario observed at a DO of 1.5 mg/L and RAS ratio of 0.5.

GRAPHICAL ABSTRACT

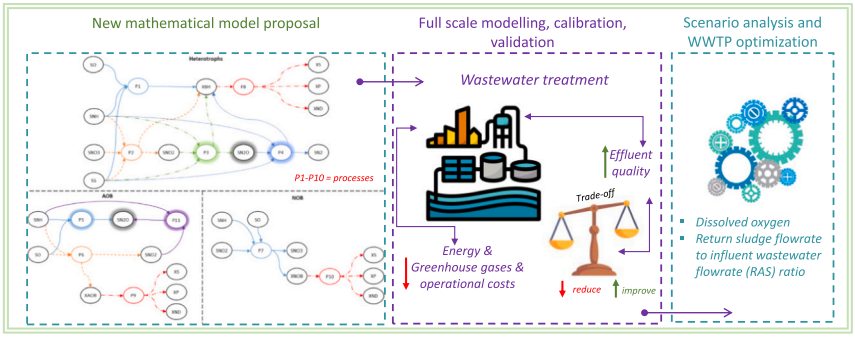

ARTICLE INFO

Editor: Pavlos Kassomenos

Keywords:
Activated sludge modelling
Carbon footprint
Nitrous oxide (N_2O)
Plant-wide modelling
Water-energy-carbon coupling index (WECCI)

ABSTRACT

Greenhouse gas (GHG) emissions from wastewater treatment plants (WWTPs) can affect climate change and must be measured and reduced. Mathematical modelling is an attractive solution to get a tool for GHG mitigation. However, although many efforts have been made to create reliable tools that can simulate "sustainable" full-scale WWTP operation, these studies are not considered complete enough to include GHG emissions and energy consumption of biological processes under long-term dynamic conditions. In this study, activated sludge model no. 1 (ASM1) was modified to model nitrous oxide (N_2O) emissions with a plant-wide modelling approach. The model is novel compared to the state of the art since it includes three steps denitrification, all N_2O production pathways and its stripping in an ASM1. The model has been calibrated and validated through long-term water quality and short-term N_2O emissions data collected from Corleone (Italy) WWTP. Different dissolved oxygen (DO) concentrations and return sludge (RAS) ratios were tested with dynamic simulations to optimise the full-scale WWTP. The scenarios have been compared synergistically with effluent quality, direct GHG emissions, and energy footprint by the water-energy-carbon coupling index (WECCI). This modelling study is novel as it fully covers long-term calibration/validation of the model with N_2O measurements and tests the dynamic optimisation. Decision-makers and operators can use this new model to optimise GHG emissions and treatment costs.

* Corresponding author.
E-mail address: alida.cosenza@unipa.it (A. Cosenza).

https://doi.org/10.1016/j.scitotenv.2023.167327
Received 19 May 2023; Received in revised form 6 September 2023; Accepted 22 September 2023
Available online 23 September 2023
0048-9697/© 2023 The Authors. Published by Elsevier B.V. This is an open access article under the CC BY-NC-ND license (http://creativecommons.org/licenses/by-nc-nd/4.0/).

1. Introduction

Greenhouse gas (GHG) emissions from wastewater treatment plants (WWTPs) (i.e., nitrous oxide (N_2O), methane (CH_4), and carbon dioxide (CO_2)) can contribute to climate change increase (Mannina et al., 2016). GHG emissions are classified as direct (related to biological processes) and indirect emissions (related to fossil fuel and electricity consumption) (Daelman et al., 2013). Direct CO_2 emissions from biogenic processes are not counted in emitted GHG from $WWTP_S$, only CO_2 gas emissions associated with fossil fuel and electricity consumption count as indirect GHG emissions (IPCC, 2022). CH_4 is released in headworks in WWTPs and anaerobic sludge treatment units (GWRC, 2011). N_2O has the highest global warming potential with 273 times CO_2 among other GHGs from WWTPs (IPCC, 2022). Therefore, special attention has been given to mitigating N_2O emissions from WWTPs (Lee et al., 2022). N_2O production pathways in biological nutrient removal systems are associated with biological nitrogen removal. Although N_2O gas is a mandatory intermediate in the denitrification process, it may not have been stripped from the liquid to gas phase directly in anoxic reactors due to the relatively high solubility of N_2O gas (GWRC, 2011). N_2O gas is an intermediate product in the nitrification reaction of autotrophic nitrifying bacteria, especially ammonia-oxidising bacteria (AOB). In addition, denitrification of AOBs involved in nitrification in activated sludge has a significant impact on N_2O production (Kim et al., 2010; Law et al., 2011; Kampschreur et al., 2009; Wunderlin et al., 2012). Although N_2O production increases with low dissolved oxygen (DO) during nitrification, aerobic conditions contribute to higher N_2O emissions due to stripping (Massara et al., 2017). Aeration is also the largest energy-consuming unit in WWTPs (Rosso et al., 2008), related to indirect emissions from WWTPs. Low carbon-nitrogen (C/N) ratios during heterotrophic denitrification and high nitrite (NO_2^-) during both nitrification and denitrification are two other factors increasing N_2O emissions from WWTPs (Mannina et al., 2017a, b). Additionally, the dynamicity of WWTPs, such as changes in anoxic/aerobic zones and influent characterisation (NH_4^+ concentration), increases N_2O production (Vasilaki et al., 2019).

N_2O emission from WWTPs can be modelled by empirical models, simplistic mass balance models, and dynamic mechanistic models (Mannina et al., 2019; Ni and Yuan, 2015). Dynamic mechanistic models that consider operational parameters effect on N_2O production predict emissions with higher accuracy. Therefore, dynamic mechanistic models are more helpful in developing emission mitigation strategies (Massara et al., 2017). Ni et al. (2013) developed a mathematical model for N_2O production by AOB and four-step heterotrophic denitrification. They calibrated and validated the model using two months of data from two WWTPs, measuring N_2O emissions from bioreactor surfaces.

DO concentration in the aerobic zone, sludge retention time (SRT), and return sludge ratio are the most critical operation parameters affecting N_2O emissions (Thakur and Medhi, 2019). Indeed, the effect and optimisation of these operational parameters to reduce N_2O accumulation have been tested by N_2O production models (Blomberg et al., 2018; Massara et al., 2018; Mannina et al., 2019; Zaborowska et al., 2019; Abulimiti et al., 2022). Blomberg et al. (2018) added N_2O production by AOBs to activated sludge model no. 3 (ASM3) and calibrated/validated their model with 17 days of dynamic data of a full-scale WWTP. They pointed out the importance of N_2O stripping models on emission estimations. Massara et al. (2018) proposed activated sludge model no. 2d (ASM2d) modification to estimate N_2O emissions from biological nitrogen and phosphorus removing WWTPs. Although Massara and co-workers showed the effect of variations of influent NH_4^+ and changing DO concentration on N_2O emissions, they did not confirm the emissions by measured data. Mannina et al. (2019) used plant-wide steady-state modelling to test the SRT, IR, and oxygen transfer efficiency (OTE) effect on the direct and indirect emissions from a full-scale WWTP. However, they did not validate the proposed model. Zaborowska et al. (2019) calibrated and validated a ASM2d + N_2O model dynamically with full-scale including N_2O measurements from a full-scale WWTP. They also tested different DO concentrations and IR ratios to mitigate N_2O emissions. However, Zaborowska et al. (2019) tested the model for 96 h of full-scale WWTP data. They analysed DO concentration and IR ratio effect on the carbon footprint (CF) of bioreactors under steady-state simulations, thus overlooking the impact of the dynamicity of WWTPs on N_2O production. Abulimiti et al. (2022) showed the importance of aeration control for balancing N_2O emissions and energy savings of WWTPs. They modified the Sumo4N model with N_2O production and tested their model with long-term data (1 year) collected from a full-scale WWTP (without N_2O measurements) and conducted sensitivity analysis before model calibration. Maktabifard et al. (2022) assessed the ASM3 + N_2O model, developed initially by Blomberg et al. (2018), and the ASM2d + N_2O model, originally developed by Zaborowska et al. (2019), on a distinct full-scale WWTP (12-days of calibration and 5-days of validation data) not previously used for validation by the original authors. They demonstrated that the AOB denitrification contribution to N_2O emissions is negligible. Solís et al. (2022) made alterations to the ASM2d-N_2O model initially proposed by Massara et al. (2018), taking into account the hydraulic conditions of the reactor. They used 3-day data from a full-scale WWTP to calibrate their modified model.

From the literature discussion presented above, one can observe that despite several efforts that have been made so far in view of setting-up reliable modelling tools able to support the "sustainable" full-scale WWTPs operation, as far as authors are aware, none of the existing include the GHG emissions, energy consumption and biological processes description under long-term dynamic conditions to ultimately

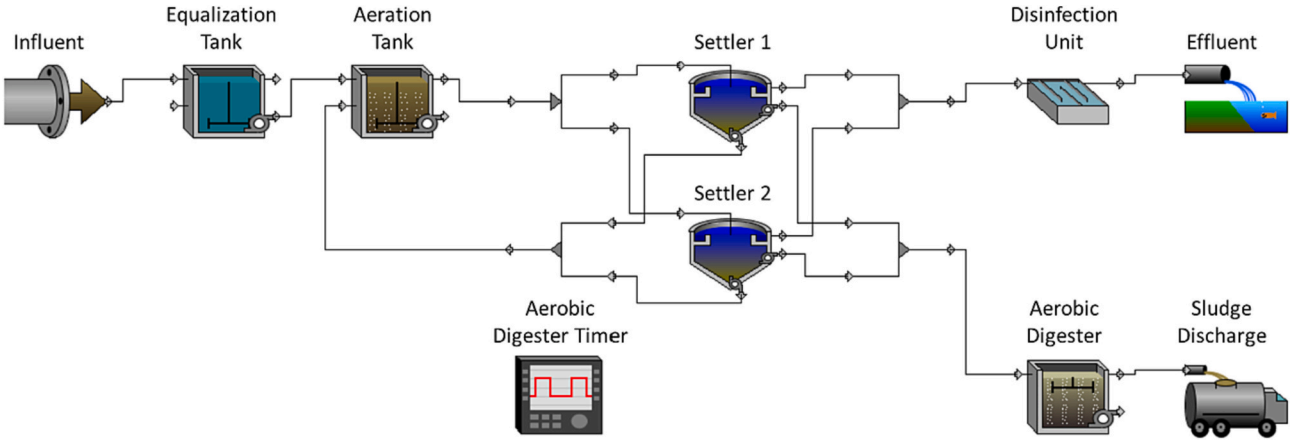

Fig. 1. Corleone WWTP layout in GPS-X.

Table 1
Sampling campaigns.

Sampling campaign	Duration	Data collection frequency	Influent	Effluent	Aeration reactor
Long term campaign	60 days	2 per week	TSS	TSS	TSS
Hourly sampling campaign−1	One day for each sampling campaign	10:00–16:00, hourly	COD	COD	TSS
Hourly sampling campaign-2			BOD_5	BOD_5	N_2O liquid
Hourly sampling campaign-3			TN	TN	N_2O gas
			NH_4-N	NH_4-N	
				NO_3-N	
				NO_2-N	

Table 2
ASM1 + N_2O model comparison with previous modelling studies.

	Hiatt and Grady (2008)	Lu et al. (2018)	Mannina et al. (2017a, b)	Mannina et al. (2018)	Zaborowska et al. (2019)	ASM1 + N_2O (This study)
	Base model					
ASM1	✓	✓	✓			✓
ASM2d				✓	✓	
Denitrification model						
4-step $S_{NO3}\rightarrow S_{NO2}\rightarrow S_{NO}\rightarrow S_{N2O}\rightarrow S_{N2}$	✓			✓		
3-step $S_{NO3}\rightarrow S_{NO2}\rightarrow S_{N2O}\rightarrow S_{N2}$		✓			✓	✓
N_2O production pathways						
Heterotrophic denitrification	✓	✓	✓	✓	✓	✓
AOB denitritation		✓		✓	✓	✓
Ammonium oxidation by AOB		✓	✓	✓	✓	✓
N_2O stripping model			✓	✓	✓	✓

highlight the trade-off between effluent quality, energy consumption, and GHG emissions in a full-scale WWTP.

In this study, activated sludge model no. 1 (ASM1) was modified to model GHG (N_2O) emissions with a plant-wide modelling approach. The model aims to estimate the effluent quality and direct and indirect emissions of a full-scale WWTP. The model was calibrated and validated via long-term water quality and short-term N_2O emission data from Corleone's WWTP (Mannina et al., 2021a, b). Optimisation scenarios with different DO concentrations and return sludge ratios were tested with dynamic simulations to optimise full-scale WWTP. Optimisation scenarios were compared, seeking a trade-off between effluent quality, energy consumption, and GHG emissions defined as the water-energy-carbon nexus (Ni et al., 2023). This new model can be used as a tool by decision-makers for designing new water reuse projects and operators for optimising treatment costs.

2. Material and methods

2.1. Characteristics of Corleone WWTP

The Corleone (Italy) WWTP has a typical Conventional Activated Sludge (CAS) process with a pre-treatment stage (sieving and degritting) and an average flow rate of 140 m^3/h (Mannina et al., 2022) (Fig. 1). The wastewater is fed to the aeration tank from equalisation with pumps. The aeration tank has fine bubble diffusers at the bottom. Concentrated sludge at the bottom of the settler is recirculated to the aeration tank. Waste sludge collected from the bottom of settlers is stabilised in an aerobic digester before discharge. The aerobic digester is aerated mechanically for 6 h a day. The effluent from settlers is disinfected by chlorine before discharge. The plant's hydraulic retention time (HRT) is 6–7 h. Flow rates of the influent wastewater, flow from the equalisation tank to the aeration tank, and return sludge from settlers to the aeration tank are measured by flowmeters.

2.2. Model development

2.2.1. Sampling campaigns

Long and short (24-h sampling) term sampling campaigns have been conducted in Corleone WWTP (Table 1) (Cosenza et al., 2023). The long-term monitoring campaign lasted for 64 days by collecting samples two times per week. Samples were collected from the influent of the aeration tank at 8 am and from the effluent at 4 pm (after one HRT has passed). Mixed liquor-suspended solid (MLSS) samples from the aeration tank were collected at 12 am. The flowrates of influent and return sludge were collected from flowmeters measured every minute in the Corleone WWTP. The influent flowrate and wastewater characterisation are given in Table 6. Auto samplers have collected samples from influent and effluent of Corleone WWTP for three different hourly sampling campaigns. The hourly sampling campaign collected N_2O samples from liquid and gas phases. Gas samples were collected using a hood (cross sectional area: 1.0 m × 0.9 m) placed on the surface of the aeration tank according to the method given in the literature (Caniani et al., 2019). An anemometer measured The gas flow rate every 30 s for the first 5 min and every minute for the last 5 min (Extech, USA). Then, gas samples were collected in Tedlar (Sensidyne, USA) gas bags using an air pump. The gas flow rate and the N_2O concentration measured in gas samples were multiplied to calculate nitrous oxide flux (Mannina et al., 2017a, b). N_2O concentration in the liquid was also measured by a micro-sensor (Unisense Environment A/S, Denmark). Liquid and gas samples were collected every hour for 6 h.

2.2.2. Biological model

N_2O emissions from biological treatment were added to ASM1 (Henze et al., 2000) by modifying N_2O emissions models provided by Hiatt and Grady (2008), Lu et al. (2018), and Zaborowska et al. (2019). The comparison of the ASM1 + N_2O model provided in this study with previous modelling studies is given in Table 2. Compared with previous literature, the model proposed here has the novelty of including all the

Table 3
ASM1 + N_2O state variables, stoichiometric and kinetic model parameters.

	Symbol	Definition	Unit
State variables	S_I	Soluble undegradable organic	g COD/m^3
	S_S	Soluble degradable organic	g COD/m^3
	X_I	Particulate undegradable organic from the influent	g COD/m^3
	X_S	Particulate degradable organic	g COD/m^3
	X_H	Heterotrophic bacteria	g COD/m^3
	X_{AOB}	Ammonia oxidising bacteria (AOB)	g COD/m^3
	X_{NOB}	Nitrite oxidising bacteria (NOB)	g COD/m^3
	X_P	Particulate undegradable endogenous products	g COD/m^3
	S_O	Dissolved oxygen	g COD/m^3
	S_{NO3}	Nitrate	g N/m^3
	S_{NO2}	Nitrite	g N/m^3
	S_{N2O}	Nitrous oxide gas (dissolved)	g N/m^3
	C_{N2O}	Nitrous oxide gas (stripped)	g N/m^3
	S_{NH}	Ammonia	g N/m^3
	X_{ND}	Particulate organic nitrogen	g N/m^3
	S_{ND}	Soluble organic nitrogen	g N/m^3
	S_{N2}	Nitrogen gas	g N/m^3
	S_{ALK}	Alkalinity	mol HCO_3^-/m^3
Stoichiometry	Y_H	Heterotrophic yield	g COD/gCOD
	Y_{AOB}	AOB yield	g COD/gCOD
	Y_{NOB}	NOB yield	g COD/gCOD
	i_{XB}	N content of active biomass	g N/g COD
	i_{SS}	N content of S_S	g N/g COD
	i_{XS}	N content of X_S	g N/g COD
	i_{XP}	N content of endogenous/inert mass	g N/g COD
	f_P	Fraction of biomass leading to particulate products	g COD/g COD
Kinetic model parameters	μ_H	Heterotrophic maximum specific growth rate	1/d
	K_S	Readily biodegradable substrate half saturation coefficient	g COD/m^3
	K_{OH}	Oxygen half saturation coefficient for growth	g O_2/m^3
	K_{NHH}	Ammonia half saturation coefficient for heterotrophic growth	g N/m^3
	η_{g1}	Anoxic growth factor (P2)	–
	K_{NO3}	Nitrate half saturation coefficient for growth	g N/m^3
	η_{g2}	Anoxic growth factor (P3)	–
	K_{NO2}	Nitrite half saturation coefficient for growth	g N/m^3
	η_{g3}	Anoxic growth factor (P4)	–
	K_{N2O}	Nitrous oxide half saturation coefficient for growth	g N/m^3
	b_H	Heterotrophic decay rate	1/d
	μ_{AOB}	AOB maximum specific growth rate	1/d
	η_{1AOB}	Ammonium oxidation pathway factor	–
	K_{OAOB}	Oxygen half saturation coefficient for AOB growth	g O_2/m^3
	K_{NHAOB}	Ammonia half saturation coefficient for AOB growth	g N/m^3
	η_{2AOB}	AOB denitrification pathway factor	–
	K_{NO2AOB}	Nitrite half saturation coefficient for AOB	g N/m^3
	b_{AOB}	AOB decay rate	1/d
	μ_{NOB}	NOB maximum specific growth rate	1/d
	K_{NO2NOB}	Nitrite half saturation coefficient for NOB	g N/m^3
	K_{ONOB}	Oxygen half-saturation coefficient for NOB growth	g O_2/m^3
	b_{NOB}	NOB decay rate	1/d
	k_a	Ammonification rate	m^3/g COD/d
	k_H	Maximum specific hydrolysis rate	1/d
	K_{OHYD}	Oxygen half saturation coefficient for hydrolysis	g O_2/m^3
	η_h	Anoxic hydrolysis factor	–
	K_{NO3HYD}	Nitrate half saturation coefficient for hydrolysis	g N/m^3
	K_{NO2HYD}	Nitrite half saturation coefficient for hydrolysis	g N/m^3
	K_{N2OHYD}	Nitrous oxide half saturation coefficient for hydrolysis	g N/m^3
	η_{ST}	Stripping reduction factor for aerobic tank	–

pathways producing N_2O, the N_2O stripping model and the 3-step denitrification in an ASM1 model. The existing ASM1 models able to describe the N_2O processes production do not include the stripping model Lu et al. (2018) and consider a simplified (2-step) denitrification process (Mannina et al., 2017a, b). The existing models providing a detailed description of the denitrification process and including all N_2O pathways (including the stripping model) are ASM2d based (Mannina et al., 2018; Zaborowska et al., 2019).

State variables, stoichiometric and kinetic model parameters are given in Table 3. The new model ASM1 + N_2O consists of 18 state variables and 19 processes.

ASM1 processes of ammonification of soluble organic nitrogen, aerobic hydrolysis, and hydrolysis of organic nitrogen remained unchanged. Ammonia switching function was added to the aerobic growth of heterotrophs as in ASM no 3 (Henze et al., 2000). Furthermore, since ammonia oxidising bacteria (AOB) are attributed to N_2O production, autotrophic biomass in ASM1 has been divided into: (i) AOB and (ii) nitrite-oxidising bacteria (NOB) (Hiatt and Grady, 2008). So, the new ASM1 + N_2O model consists of heterotrophic, ammonia-oxidising, and nitrite-oxidising biomass.

Fig. 2 summarises the growth and decay processes of biomass included in the ASM1 + N_2O model. Heterotrophic growth under anoxic conditions (denitrification was modelled in 3-steps (Lu et al., 2018): (Process 2 (P2)) from nitrate (S_{NO3}) to nitrite (S_{NO2}), (Process 3 (P3)) from S_{NO2} to nitrous oxide (S_{N2O}), and (Process 4 (P4)) from S_{N2O} to nitrogen gas (S_{N2}). The 3-step double-pathway N_2O model by AOB was implemented to ASM1 according to Lu et al. (2018): (Process 5 (P5)) ammonium (S_{NH}) oxidation to S_{N2O} (hydroxylamine oxidation), (Process 6 (P6)) S_{NH} oxidation to S_{NO2} (nitritation), and (Process 11 (P11)) S_{NO2} reduction to S_{N2O} (AOB denitrification) (S_{NH} is the electron donor). Anoxic hydrolysis is also divided into three processes each has a different electron (e^-) acceptor (P14, P15, and P16). The transition from dissolved N_2O gas to the was modelled by the N_2O stripping model given by Schulthess and Gujer (1996) for both anoxic and aerobic conditions. However, a stripping reduction factor was defined for aerobic stripping (η_{ST}) to reflect the non-ideality of the stripping model (Massara et al., 2018). Alkalinity (S_{ALK}) was added as a component to check the continuity of the model and was verified as proposed by Hauduc et al. (2010). The model matrix is given in Table 5.

2.2.3. Model application and calibration

Model application and calibration steps are given in Fig. 3. Corleone WWTP layout (Fig. 1) was implemented in GPS-X simulation software 7.0 (Hydromantis). The model has been constructed by using the Model

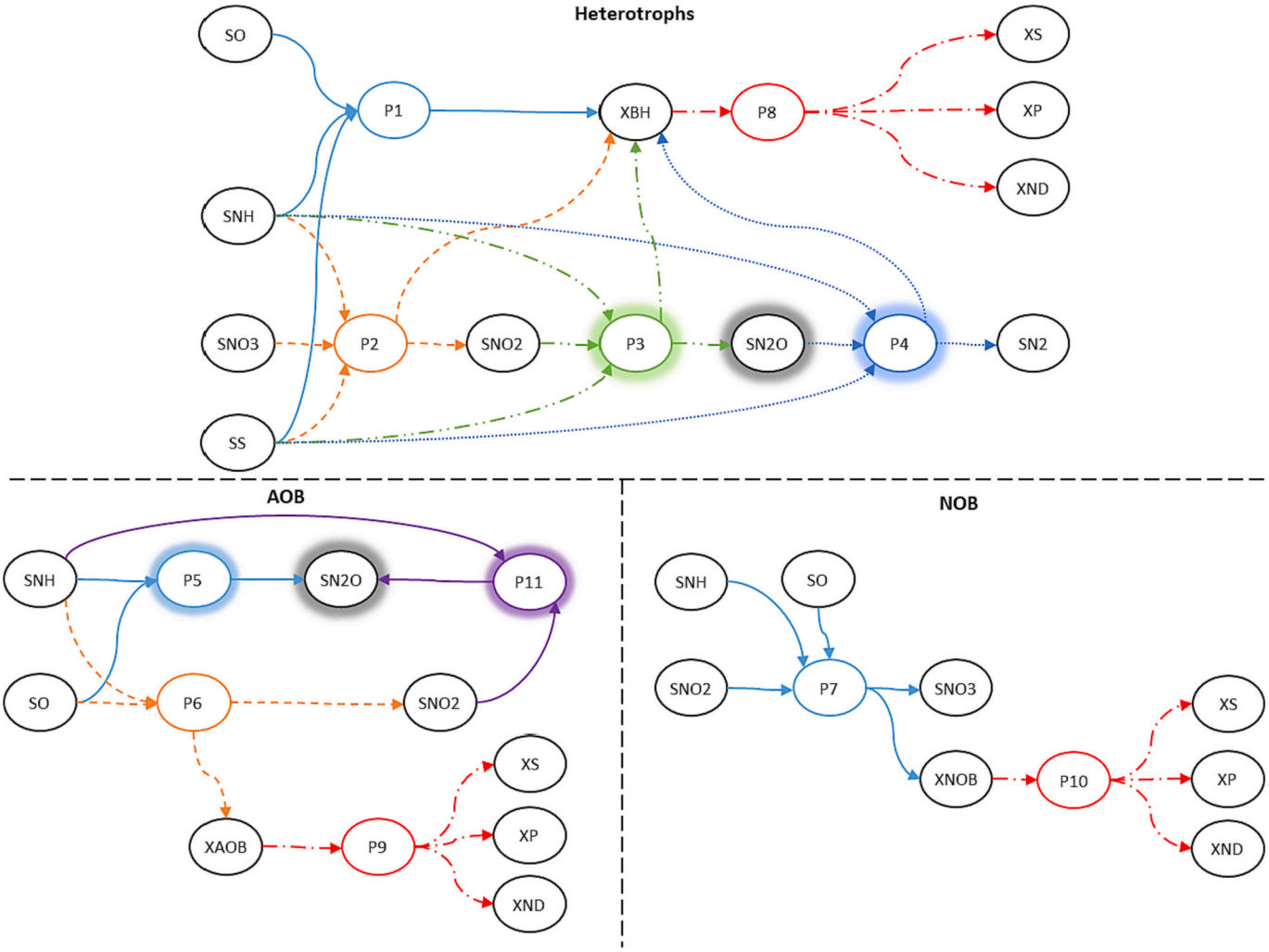

Fig. 2. Growth, decay, and N_2O producing processes: P1: Aerobic growth of heterotrophs; P2: Anoxic growth of heterotrophs (S_{NO3}→S_{NO2}); P3: Anoxic growth of heterotrophs (S_{NO2}→S_{N2O}); P4: Anoxic growth of heterotrophs (S_{N2O}→S_{N2}); P5: Ammonium oxidation; P6: Aerobic growth of AOBs (Nitritation); P7: Aerobic growth of NOBs; P8: Decay of heterotrophs; P9: Decay of AOBs; P10: Decay of NOBs; P11: AOB Denitrification.

Developer tool in GPS-X. The carbon-nitrogen-industrial (cnip) library was selected including X_{AOB}, X_{NOB}, S_{NO3}, S_{NO2}, S_{N2O}, and C_{N2O} state variables. The representative model outputs and calibration sequence were defined, then the range of model parameters was determined according to the literature. Model calibration was done using Corleone WWTP's dynamic 30-day data and validated different 30-day data of Corleone WWTP. Calibration was done by Optimizer Tool in GPS-X by selecting maximum likelihood as an objective function (Mannina and Cosenza, 2015). N_2O concentration in the liquid and gas phases was calibrated according to the hourly sampling campaign. Direct GHG emissions were calculated by multiplying gas N_2O concentration and air flow rates measured during the hourly sampling campaign. The energy consumption of pumps and blower were defined in GPS-X.

The model's goodness-of-fit was expressed in the normalised mean of absolute errors (NMAE) (Eq. (1)) and normalised root of mean squared errors (NRMSE) (Eq. (2)). Where y_o and y_s are observed and simulated model outputs, respectively. $y_{o,mean}$ the mean value of the observed model outputs (Table 4).

$$NMAE = \frac{\frac{1}{n}\sum_{i=1}^{n}|y_o - y_s|}{y_{o,mean}} \quad (1)$$

$$NRMSE = \frac{\sqrt{\frac{\sum_{i=1}^{n}(y_o - y_s)^2}{n}}}{y_{o,mean}} \quad (2)$$

2.2.4. WWTP influent model

Influent concentrations measured in hourly and long-term sampling campaigns were used to create minutely dynamic wastewater characterisation in Fourier series according to the literature (Mannina et al., 2011). More precisely, the parameters of a truncated Fourier series were first calibrated starting from discrete hourly measured data. Then, the long-term measured data were adopted to generate the dynamic influent series for 64 days simulations. Specifically, each long-term discrete data was adopted to generate the daily average trend by using a linear relationship to avoid discontinuities according to (Mannina et al., 2011). Then, knowing the average daily patter for each state variable and the long-term data the calibrated Fourier series was extended to the 64 days. The average daily flowrate and characterisation of the influent wastewater monitored for the long term is given in Table 6.

2.2.5. Optimisation scenarios

Operational parameters of DO concentration in the aeration tank and the return sludge flowrate to influent wastewater flowrate (RAS) ratio were tested in nine different operation scenarios. Scenarios were run

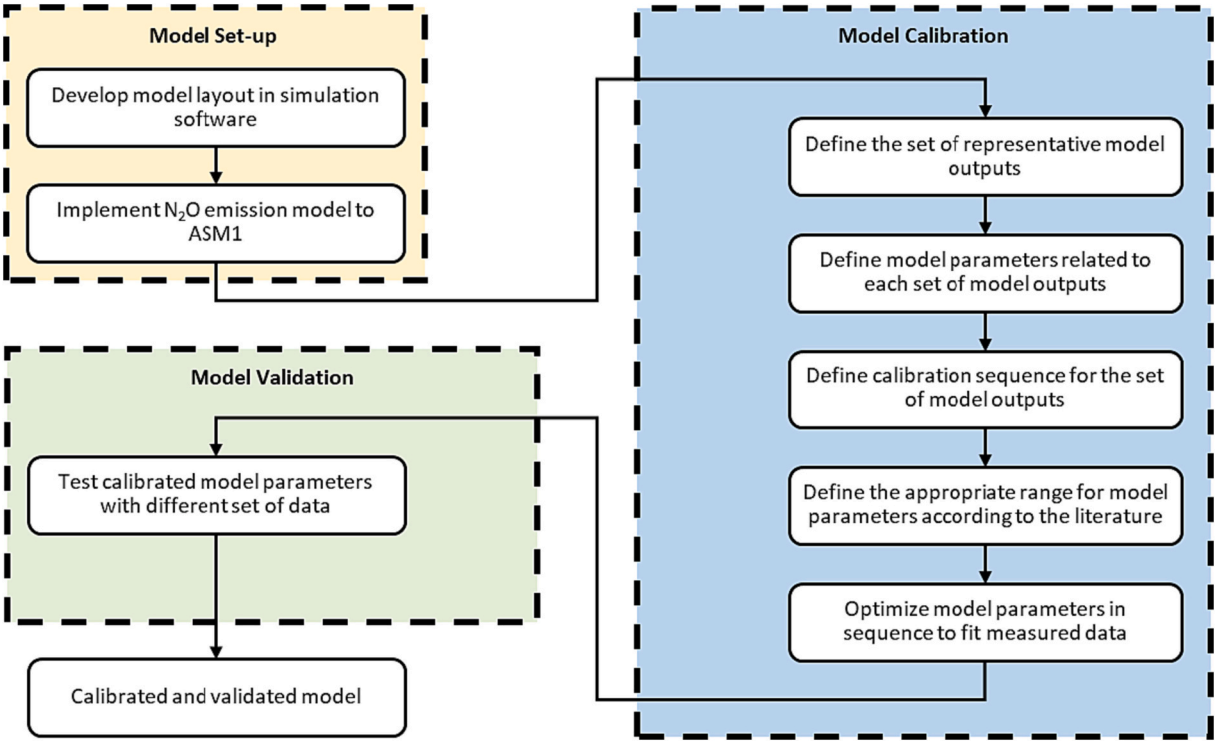

Fig. 3. Model application and calibration steps.

with 60 days of data collected in a long-term sampling period. The baseline scenario (S0) reflects the existing situation of the Corleone WWTP (DO = 2 mg/L and RAS = 66 % of influent flow rate). Table 7 summarises nine operational scenarios tested with the dynamic simulation of the calibrated ASM1 + N_2O model.

Operation scenarios were compared using an index considering water (effluent quality), N_2O emissions, and energy consumption. Ni et al. (2023) provided the water-energy-carbon coupling index (WECCI) as a tool that combines different dimensional measures into one index for multi-objective trade-offs. In WECCI, water quality is measured by grey water footprint (GWF), defined as freshwater required to absorb pollutant loads according to receiving water body standards (Arjen et al., 2012). Energy footprint (ENF) is estimated by the overall energy consumption of WWTPs. Finally, CF is estimated according to the Greenhouse Gas Protocol, which calculates direct emissions (scope 1), indirect emissions from the purchase of electricity (scope 2), and indirect emissions from chemical consumption (scope 2) (World Resource Institute, 2014). In this paper, the WECCI calculation given by Ni et al. (2023) has been modified:

- Water quality is measured by the effluent quality index (EQI) instead of GWF.
- Only direct GHG emissions from wastewater treatment have been counted for CF.
- Calibrated ASM1 + N2O model of the WWTP estimated direct emissions (N2O emissions).
- ENF was calculated based on the electricity consumption of the WWTP.

The EQI is a simple tool used in benchmark studies to compare the treatment performance of WWTPs based on pollutant load in the effluent (Copp, 2002). On the other hand, GWF calculations are based on the discharge limit and the pollutant absorption capacity of the receiving water body, thus requiring information about the receiving body and the standards that WWTP must comply with. GPS-X calculates EQI by Eq. (3) given in Copp (2002). Q is the instantaneous flowrate (m^3/d), n is the number of compounds, w_i is the weight factor of the compound, $S_i(t)$ is the instantaneous concentration of the compound. The selected compounds for EQI (kg pollutant/day) estimation are TSS, COD, BOD_5, and TN and the weight factors are 2, 1, 2, and 20, respectively.

$$EQI = Q(t)\sum_{i=1}^{n} w_i \bullet S_i(t) \tag{3}$$

Only direct GHG emissions from WWTP have been counted for CF because for a WWTP that only purchases electricity and does not produce it internally from biogas, the ENF and scope 2 of CF represent the electricity consumption of the WWTP and are thus counted twice in the WECCI. To prevent this, electricity consumption was taken into account in ENF, while direct emissions were counted in CF. ENF (kWh/m^3) was calculated by dividing energy consumption (kWh/d) by influent flowrate (m^3/d) Ni et al. (2023). CF was calculated by dividing N_2O emission (g/d) by influent wastewater flowrate (m^3/d). N_2O emission (g/d) was calculated by multiplying N_2O concentration (g/m^3) in the gas form and airflow to the aeration tank (m^3/d). Afterward, EQI, CF, and ENF were subjected to normalisation using Eq. (4) (Ni et al., 2023), so the range is between 0 and 1. A' is the normalised EQI, CF, or ENF. Max(A) and Min (A) are the maximum and minimum values of the EQI, CF, or ENF. The WECCI was then computed by summing up the normalised EQI, CF, and ENF values.

$$A' = \frac{max(A) - A}{max(A) - min\,(A)} \tag{4}$$

3. Results and discussion

3.1. WWTP influent model

Corleone WWTP's measured influent characterisation data during hourly sampling campaigns were used to estimate the Fourier series parameters. The parameters were adjusted to minimise the sum of squared errors. The generated long-term input time series are given in Fig. 4.

Table 4
ASM1 + N_2O processes and rate equations.

Code	Process	Rate equation
P1	Aerobic growth of heterotrophs	$\mu_H \bullet \left(\frac{S_S}{K_S + S_S}\right) \bullet \left(\frac{S_O}{K_{OH} + S_O}\right) \bullet \left(\frac{S_{NH}}{K_{NHH} + S_{NH}}\right) \bullet X_H$
P2	Anoxic growth of heterotrophs (S_{NO3}→S_{NO2})	$\mu_H \bullet \eta_{g1} \bullet \left(\frac{S_S}{K_S + S_S}\right) \bullet \left(\frac{K_{OH}}{K_{OH} + S_O}\right) \bullet \left(\frac{S_{NO3}}{K_{NO3} + S_{NO3}}\right) \bullet \left(\frac{S_{NH}}{K_{NHH} + S_{NH}}\right) \bullet X_H$
P3	Anoxic growth of heterotrophs (S_{NO2}→S_{N2O})	$\mu_H \bullet \eta_{g2} \bullet \left(\frac{S_S}{K_S + S_S}\right) \bullet \left(\frac{K_{OH}}{K_{OH} + S_O}\right) \bullet \left(\frac{S_{NO2}}{K_{NO2} + S_{NO2}}\right) \bullet \left(\frac{S_{NH}}{K_{NHH} + S_{NH}}\right) \bullet X_H$
P4	Anoxic growth of heterotrophs (S_{N2O}→S_{N2})	$\mu_H \bullet \eta_{g3} \bullet \left(\frac{S_S}{K_S + S_S}\right) \bullet \left(\frac{K_{OH}}{K_{OH} + S_O}\right) \bullet \left(\frac{S_{N2O}}{K_{N2O} + S_{N2O}}\right) \bullet \left(\frac{S_{NH}}{K_{NHH} + S_{NH}}\right) \bullet X_H$
P5	Ammonium oxidation	$\mu_{AOB} \bullet \eta_{1AOB} \bullet \left(\frac{S_O}{K_{OAOB} + S_O}\right) \bullet \left(\frac{S_{NH}}{K_{NHAOB} + S_{NH}}\right) \bullet X_{AOB}$
P6	Aerobic growth of AOBs (Nitritation)	$\mu_{AOB} \bullet \left(\frac{S_O}{K_{OAOB} + S_O}\right) \bullet \left(\frac{S_{NH}}{K_{NHAOB} + S_{NH}}\right) \bullet X_{AOB}$
P7	Aerobic growth of NOBs	$\mu_{NOB} \bullet \left(\frac{S_{NO2}}{K_{NO2NOB} + S_{NO2}}\right) \bullet \left(\frac{S_O}{K_{ONOB} + S_O}\right) \bullet X_{NOB}$
P8	Decay of heterotrophs	$b_H \bullet X_H$
P9	Decay of AOBs	$b_{AOB} \bullet X_{AOB}$
P10	Decay of NOBs	$b_{NOB} \bullet X_{NOB}$
P11	AOB Denitrification	$\mu_{AOB} \bullet \eta_{2AOB} \bullet \left(\frac{K_{OAOB}}{K_{OAOB} + S_O}\right) \bullet \left(\frac{S_{NH}}{K_{NHAOB} + S_{NH}}\right) \bullet \left(\frac{S_{NO2}}{K_{NO2AOB} + S_{NO2}}\right) \bullet X_{AOB}$
P12	Ammonification of soluble organic nitrogen	$k_a \bullet S_{ND} \bullet X_H$
P13	Aerobic hydrolysis	$k_H \bullet \left(\frac{\frac{X_S}{X_H}}{K_X + \frac{X_S}{X_H}}\right) \bullet \left(\frac{S_O}{K_{OHYD} + S_O}\right) \bullet X_H$
P14	Anoxic hydrolysis (S_{NO3} is the e^- acceptor)	$k_H \bullet \eta_h \bullet \left(\frac{\frac{X_S}{X_H}}{K_X + \frac{X_S}{X_H}}\right) \bullet \left(\frac{K_{OHYD}}{K_{OHYD} + S_O}\right) \bullet \left(\frac{S_{NO3}}{K_{NO3HYD} + S_{NO3}}\right) \bullet X_H$
P15	Anoxic hydrolysis (S_{NO2} is the e^- acceptor)	$k_H \bullet \eta_h \bullet \left(\frac{\frac{X_S}{X_H}}{K_X + \frac{X_S}{X_H}}\right) \bullet \left(\frac{K_{OHYD}}{K_{OHYD} + S_O}\right) \bullet \left(\frac{S_{NO2}}{K_{NO2HYD} + S_{NO2}}\right) \bullet X_H$
P16	Anoxic hydrolysis (S_{N2O} is the e^- acceptor)	$k_H \bullet \eta_h \bullet \left(\frac{\frac{X_S}{X_H}}{K_X + \frac{X_S}{X_H}}\right) \bullet \left(\frac{K_{OHYD}}{K_{OHYD} + S_O}\right) \bullet \left(\frac{S_{N2O}}{K_{N2OHYD} + S_{N2O}}\right) \bullet X_H$
P17	Hydrolysis of organic nitrogen	$k_H \bullet \left(\frac{\frac{X_S}{X_H}}{K_X + \frac{X_S}{X_H}}\right) \bullet \left(\frac{S_O}{K_{OHYD} + S_O}\right) \bullet X_H \bullet \left(\frac{X_{ND}}{X_S}\right)$
P18	Anoxic S_{N2O} stripping	$Kla_{N2OAN} * \left(S_{N2O} - \left(\frac{c_{N2OAIR}}{H_{N2O}}\right)\right)$
P19	Aerobic S_{N2O} stripping	$H_{N2O} \bullet S_{N2O} \bullet \left(1 - e^{-\left(\frac{Kla_{N2O}}{H_{N2O}} \times \frac{V}{Q_A}\right)}\right) \bullet \left(\frac{Q_A}{V}\right) \bullet \eta_{ST}$

3.2. Model calibration

MLSS and COD, NH_4-N, NO_2-N, and NO_3-N in the effluent were selected as representative model outputs and calibrated in this order. For MLSS calibration, WAS flow rates were arranged, then heterotrophic yield (Y_H) was optimised. Heterotrophic maximum specific growth rate (μ_H) biomass kinetic coefficients were optimised for effluent COD concentration. For effluent NH_4-N, DO concentration in the aeration tank was arranged. Then AOB's maximum specific growth rate (μ_{AOB}) and ammonia half saturation coefficient for AOB growth (K_{NHAOB}) were optimised according to effluent NH_4-N concentration. For NO_3-N, NOB's maximum specific growth rate (μ_{NOB}), oxygen half saturation coefficient for NOB and heterotrophic growth (K_{ONOB} and K_{OH}, respectively), and anoxic growth factors of heterotrophs (η_{g1}, η_{g2}, and η_{g3}) were optimised. For N_2O concentrations in liquid and in the gas phase in the aerobic reactor, the ammonium oxidation pathway factor (η_{1AOB}) and AOB denitrification pathway factor (η_{2AOB}) were optimised.

Table 8 shows calibrated ASM1 + N_2O kinetic parameters to fit COD, NH_4-N, NO_3-N, and NO_2-N concentrations in the effluent of Corleone WWTP. Heterotrophic biomass activity had to be lowered to the effluent COD concentration with the measured data by increasing the decay rate (b_H). The average NH_4-N concentration in the effluent was 3.9 ± 2.4 mg/L, indicating that nitrification was not completed most of the time. Thus, AOBs activity was reduced by arranging the maximum specific growth rate (μ_{AOB}) and oxygen half saturation coefficient for growth (K_{OAOB}) as 0.55 1/d and 0.9 g O_2/m^3, respectively. The average NO_2-N and NO_3-N concentrations were 0.1 ± 0.09 mg/L and 8.3 ± 4.4 mg/L, suggesting that NO_2-N was not accumulated but converted to NO_3-N by NOBs. Therefore, NOBs' maximum growth rate (μ_{NOB}) was increased to 1.32 1/d. N_2O stripping from liquid to air had to be decreased so the stripping reduction factor for the aerobic tank (η_{ST}) was arranged as 0.2.

Fig. 5 shows calibration and validation simulation results in comparison to measured data in the effluent of Corleone WWTP. It can be seen that the model correctly describes the trend of COD in the effluent. NH_4-N concentrations in the effluent are given in Fig. 5 (b) and (f) for calibration and validation period, respectively. It was assumed that high NH_4-N concentrations in the effluent indicated the low dissolved oxygen concentrations in the aeration tank that limits nitrification. When DO concentration is low, heterotrophic denitrification activity increases. For instance, between 0 and 8 days, the influent NH_4-N concentration was 16 ± 3.9 mg/L in average, in the effluent, NH_4-N concentrations were over 4 mg/L and NO_3-N concentrations were below 6 mg/L. This indicates heterotrophic denitrification. So, especially when DO concentration was below 1 mg/L, heterotrophic activity affected NO_2-N and NO_3-N concentrations in the effluent due to heterotrophic denitrification. Therefore, kinetic parameters were arranged to fit the trade-off between effluent COD and oxidised nitrogen concentrations.

During the calibration period, the NMAE for COD, NH_4-N, NO_2-N,

Table 5
ASM1 + N_2O model stoichiometric matrix.

Process	S_I	S_S	X_I	X_S	X_H	X_{AOB}	X_{NOB}	X_P	S_O	S_{NO3}	S_{NO2}	S_{N2O}	C_{N2O}	S_{NH}	S_{ND}	X_{ND}	S_{N2}	S_{ALK}
1		$-\frac{1}{Y_H}$			1				$-\frac{1-Y_H}{Y_H}$					$-i_{XB}$				$-i_{XB}\cdot icharge_{NH4}$
2		$-\frac{1}{Y_H}$			1					$\frac{(1-Y_H)}{(icod_{NO3}-icod_{NO2})\cdot Y_H}$	$-\frac{(1-Y_H)}{(icod_{NO3}-icod_{NO2})\cdot Y_H}$			$-i_{XB}$				$\left(\frac{(1-Y_H)}{(icod_{NO3}-icod_{NO2})\cdot Y_H}\right)\cdot icharge_{NO3}$ $+\left(-\frac{(1-Y_H)}{(icod_{NO3}-icod_{NO2})\cdot Y_H}\right)\cdot icharge_{NO2}$ $+(-i_{XB})\cdot icharge_{NH4}$
3		$-\frac{1}{Y_H}$			1						$\frac{(1-Y_H)}{(icod_{NO2}-icod_{N2O})\cdot Y_H}$	$-\frac{(1-Y_H)}{(icod_{NO2}-icod_{N2O})\cdot Y_H}$		$-i_{XB}$				$\left(\frac{(1-Y_H)}{(icod_{NO2}-icod_{N2O})\cdot Y_H}\right)\cdot icharge_{NO2}+(-i_{XB})$ $\cdot icharge_{NH4}$
4		$-\frac{1}{Y_H}$			1							$\frac{(1-Y_H)}{(icod_{N2O}-icod_{N2})\cdot Y_H}$		$-i_{XB}$			$-\frac{(1-Y_H)}{(icod_{N2O}-icod_{N2})\cdot Y_H}$	$-i_{XB}\cdot icharge_{NH4}$
5									$icod_{N2O}$			1		-1				$-icharge_{NH4}$
6						1			$-\frac{-icod_{NO2}-Y_{AOB}}{Y_{AOB}}$		$\frac{1}{Y_{AOB}}$			$-i_{XB}-\frac{1}{Y_{AOB}}$				$\left(\frac{1}{Y_{AOB}}\right)\cdot icharge_{NO2}+\left(-i_{XB}-\frac{1}{Y_{AOB}}\right)\cdot icharge_{NH4}$
7							1		$-\frac{-icod_{NO3}+icod_{NO2}-Y_{NOB}}{Y_{NOB}}$	$\frac{1}{Y_{NOB}}$	$-\frac{1}{Y_{NOB}}$			$-i_{XB}$				$\left(-\frac{1}{Y_{NOB}}\right)\cdot icharge_{NO2}+(-i_{XB})\cdot icharge_{NH4}$
8				$1-f_P$	-1			f_P								$i_{XB}-f_P\cdot i_{XP}$		
9				$1-f_P$		-1		f_P								$i_{XB}-f_P\cdot i_{XP}$		
10				$1-f_P$			-1	f_P								$i_{XB}-f_P\cdot i_{XP}$		
11											-2	3		-1				$(-2)\cdot icharge_{NO2}-icharge_{NH4}$
12														1	-1			$icharge_{NH4}$
13		1		-1										$-(i_{SS}-i_{XS})$				
14		1		-1										$-(i_{SS}-i_{XS})$				
15		1		-1										$-(i_{SS}-i_{XS})$				
16		1		-1										$-(i_{SS}-i_{XS})$				
17															1	-1		
18												-1	1					
19												-1	1					

Symbol	*Conservation factor*	*Unit*	*Value*
$icod_{NO3}$	*for nitrate in COD*	*g COD/g N*	*-4.571*
$icod_{NO2}$	*for nitrite in COD*	*g COD/g N*	*-3.429*
$icod_{N2O}$	*for nitrous oxide in COD*	*g COD/g N*	*-2.286*
$icod_{N2}$	*for nitrogen in COD*	*g COD/g N*	*-1.714*
$icharge_{NH4}$	*for ammonium in charge*	*Charge/g N*	*0.071*
$icharge_{NO3}$	*for nitrate in charge*	*Charge/g N*	*-0.071*
$icharge_{NO2}$	*for nitrite in charge*	*Charge/g N*	*-0.071*

Table 6
Influent characterisation.

	Daily flowrate (m^3/d)	COD (mg/L)	BOD_5 (mg/L)	TN (mg/L)	NH_4-N (mg/L)
Average	2674	219	85	26.4	24.1
Standard deviation	484	76	49	4.9	4.7
Minimum	1589	109	18	18.2	16.0
Maximum	3271	383	184	33.0	30.3
Number of data	64	17	17	17	17

Table 7
Operation scenarios.

	The RAS ratio is set to 0.5	The RAS ratio is set to 0.75	The RAS ratio is set to 1
DO is set to 1 mg/L	S1	S2	S3
DO is set to 1.5 mg/L	S4	S5	S6
DO is set to 2 mg/L	S7	S8	S9

and NO_3-N were 0.25, 0.28, 0.71, and 0.38, respectively. In the validation period, the NMAE values for the same parameters were 0.21, 0.39, 0.39, and 0.54, respectively. In the calibration period, the NRMSE values for COD, NH_4-N, NO_2-N, and NO_3-N were 0.26, 0.34, 0.87, and 0.51, respectively. In the subsequent validation period, these NRMSE values for the same model outputs were 0.22, 0.49, 0.53, and 0.67. Lower NMAE and NRMSE values indicate better model performance and a closer fit between simulated and observed data. The model exhibited the highest accuracy when predicting effluent COD concentration and the worst performance when estimating effluent NO_2-N concentration (Fig. 6).

Table 8
Calibrated model parameters.

Symbol	Unit	ASM1	Hiatt and Grady (2008)	Lu et al. (2018)	Zaborowska et al. (2019)	This study
Y_H	g COD/gCOD	0.67	0.6	0.6	0.63	0.706
Y_{AOB}	g COD/gCOD	–	0.18	0.18	0.15	0.15
Y_{NOB}	g COD/gCOD	–	0.06	0.06	0.06	0.06
i_{XB}	g N/g COD	0.086	0.086	0.07	0.04	0.086
i_{SS}	g N/g COD	–	–	–	–	0.03
i_{XS}	g N/g COD	–	–	–	–	0.04
i_{XP}	g N/g COD	0.06	0.06	0.06	0.02	0.06
f_P	g COD/g COD	0.08	0.08	0.08	0.1	0.08
μ_H	1/d	6	6.25	6.25	3	2.906
K_S	g COD/m^3	20	20	20	–	20
K_{OH}	g O_2/m^3	0.2	0.1	0.1	0.3	0.375
K_{NHH}	g N/m^3	–	–	0.05	0.02	0.02
η_{g1}	–	0.8	0.8	0.03	0.8	0.561
K_{NO3}	g N/m^3	0.5	0.2	0.2	0.5	0.2
η_{g2}	–	–	0.28	0.16	0.6	0.16
K_{NO2}	g N/m^3	–	0.2	0.2	0.5	0.2
η_{g3}	–	–	–	0.35	0.25	0.173
K_{N2O}	g N/m^3	–	0.05	0.05	0.035	0.05
b_H	1/d	0.62	0.408	0.408	0.4	0.8
μ_{AOB}	1/d	–	0.78	0.78	1.1	0.561
η_{1AOB}	–	–	–	0.8	0.2	0.4
K_{OAOB}	g O_2/m^3	–	0.6	0.6	0.5	0.9
K_{NHAOB}	g N/m^3	–	0.1	1	1.2	1.212
η_{2AOB}	–	–	–	0.074	0.07	0.07
K_{NO2AOB}	g N/m^3	–	–	8	8	8
b_{AOB}	1/d	–	0.096	0.096	0.15	0.15
μ_{NOB}	1/d	–	0.78	0.78	1	1.32
K_{NO2NOB}	g N/m^3	–	–	0.5	0.5	0.5
K_{ONOB}	g O_2/m^3	–	1.2	0.68	0.68	0.666
b_{NOB}	1/d	–	0.096	0.096	0.06	0.06
k_a	m^3/g COD/d	0.08	0.1608	0.08	–	0.08
k_H	1/d	3	2.208	3	2.5	3
K_{OHYD}	g O_2/m^3	0.2	0.1	–	0.2	0.2
η_h	–	0.4	–	0.4	0.4	0.4
K_{NO3HYD}	g N/m^3	0.5	–	–	0.5	0.5
K_{NO2HYD}	g N/m^3	–	–	–	0.5	0.5
K_{N2OHYD}	g N/m^3	–	–	–	0.5	0.5
η_{ST}	–	–	–	–	–	0.2

Table 9
EQI, CF, and ENF values per m_3 of wastewater for each scenario.

		EQI (kg/m^3)			CF (mg/m^3)			ENF (kWh/m^3)		
		RAS ratio			RAS ratio			RAS ratio		
		0.5	0.75	1	0.5	0.75	1	0.5	0.75	1
DO	1 mg/L	0.193	0.199	0.203	***0.546***	0.556	0.557	***0.137***	0.142	0.147
	1.5 mg/L	0.151	0.152	0.153	0.571	0.587	0.593	0.145	0.150	0.156
	2 mg/L	0.139	***0.138***	0.139	0.622	0.640	0.646	0.151	0.157	0.163

3.3. Scenarios

The average EQI of Corleone WWTP was 471 kg/day. The specific EQI, ENF, and CF were 0.176 kg/m^3, 0.147 kWh/m^3, and 0.814 mg/m^3, respectively. The direct GHG emissions from Corleone WWTP were calculated as 0.58 kg CO_2 eq/d while indirect GHG emissions were 0.27 kg CO_2 eq/d. Direct emissions were responsible for 68 % of the total GHG emissions from Corleone WWTP. For a nutrient removing activated sludge system (such as A_2O), Zaborowska et al. (2019) found this ratio as between 51 and 80 %.

The specific EQI, ENF, and CF per m^3 of wastewater for each scenario are given in Table 9. The minimum EQI of 0.138 kg/m^3 was achieved when DO was 2 mg/L and RAS was 0.75. Compared to the baseline scenario (DO of 2 mg/L and RAS ratio of 0.66), a 21 % of decrease was achieved in EQI. This is because in the scenario run in the model the DO concentration was kept at 2 mg/L with 0.5 mg/L of off-set value, but in the baseline scenario (actual situation in the WWTP) the DO concentration was manually regulated by the operator through adjustments to the aeration rate in the reactor. As a result, it appears that the automatic DO control led to an improvement in effluent quality. Compared to the baseline scenario, the CF was decreased to 0.546 mg/m^3 (33%) when DO was 1 mg/L and RAS ratio was 0.5. Because both direct and indirect N_2O emissions were decreased (32 % and 7 %, respectively) with decreased DO concentration and RAS ratio. Similarly, the lowest ENF (0.137 kWh/m^3) was observed when DO was 1 mg/L and RAS ratio was 0.5. This 7 % decrease in ENF was contributed to the energy savings due to lowered aeration and pumping energy consumptions compared to the baseline scenario.

Different DO concentration and RAS ratios were simulated to compare their effects on WECCI, including EQI, CF, and ENF. Fig. 7 summarises nine scenarios. From Fig. 7 (a), it can be seen that DO concentration is very effective on EQI. Indeed, the lowest normalised EQI was observed when the DO concentration was 1 mg/L and increased with increasing DO concentration. Because increase in DO concentration increases the oxidation of organics and nitrification, thus better quality is observed in the effluent. It is worth noting that the RAS ratio is more effective on the EQI at lower DO concentrations. When DO was 1 mg/L, the increase in RAS ratio from 0.5 to 1 decreased normalised EQI from 0.15 to 0. On the other hand, the same increase in RAS ratio decreased normalised EQI from 1 to 0.99 when DO concentration was 2 mg/L. Therefore, the best operation scenario for the highest normalised EQI is a DO concentration of 2 mg/L and an RAS ratio of 0.75.

Fig. 7 (b) shows how normalised CF is affected by changes in DO concentration and RAS ratio. The best scenario for the highest normalised CF was observed at a DO concentration of 1 mg/L and RAS ratio of 0.5. Since CF is related to N_2O emissions from the aeration tank, the scenario with the lowest aeration gave the best result since it has the least stripping N_2O from the liquid. Therefore, DO concentration is more effective on the CF than the RAS ratio. Under the RAS ratio of 0.75, an increase in DO concentration from 1 mg/L to 2 mg/L caused a decrease in normalised CF from 0.9 to 0.06. On the other hand, at a DO concentration of 1.5 mg/L, the increase in RAS ratio from 0.5 to 1 decreased normalised CF from 0.75 to 0.53. Zaborowska et al. (2019) also tested DO concentration and RAS ratio effect on CF from bioreactors and found the optimum condition as 1.3 g/L of DO concentration and 0.73 of RAS ratio considering N_2O emissions and energy consumption from activated sludge system with pre-denitrification (A^2O). Fig. 7 (c) shows the normalised ENF change with changing DO concentration and RAS ratio. Since DO concentration and RAS ratio are related to energy consumption of the plant, both operational conditions were effective on ENF. Indeed, the best normalised ENF was observed when DO concentration and RAS ratio were the lowest, 1 mg/L and 0.5, respectively.

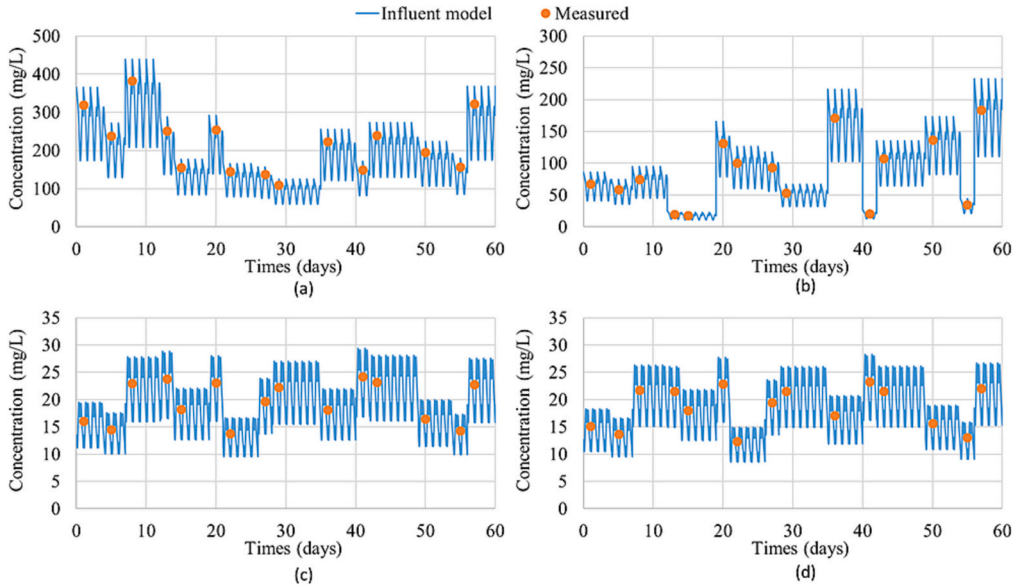

Fig. 4. Measured and generated according to Fourier series influent characterisation of Corleone WWTP: (a) COD, (b) BOD_5, (c) TN, (d) NH_4-N.

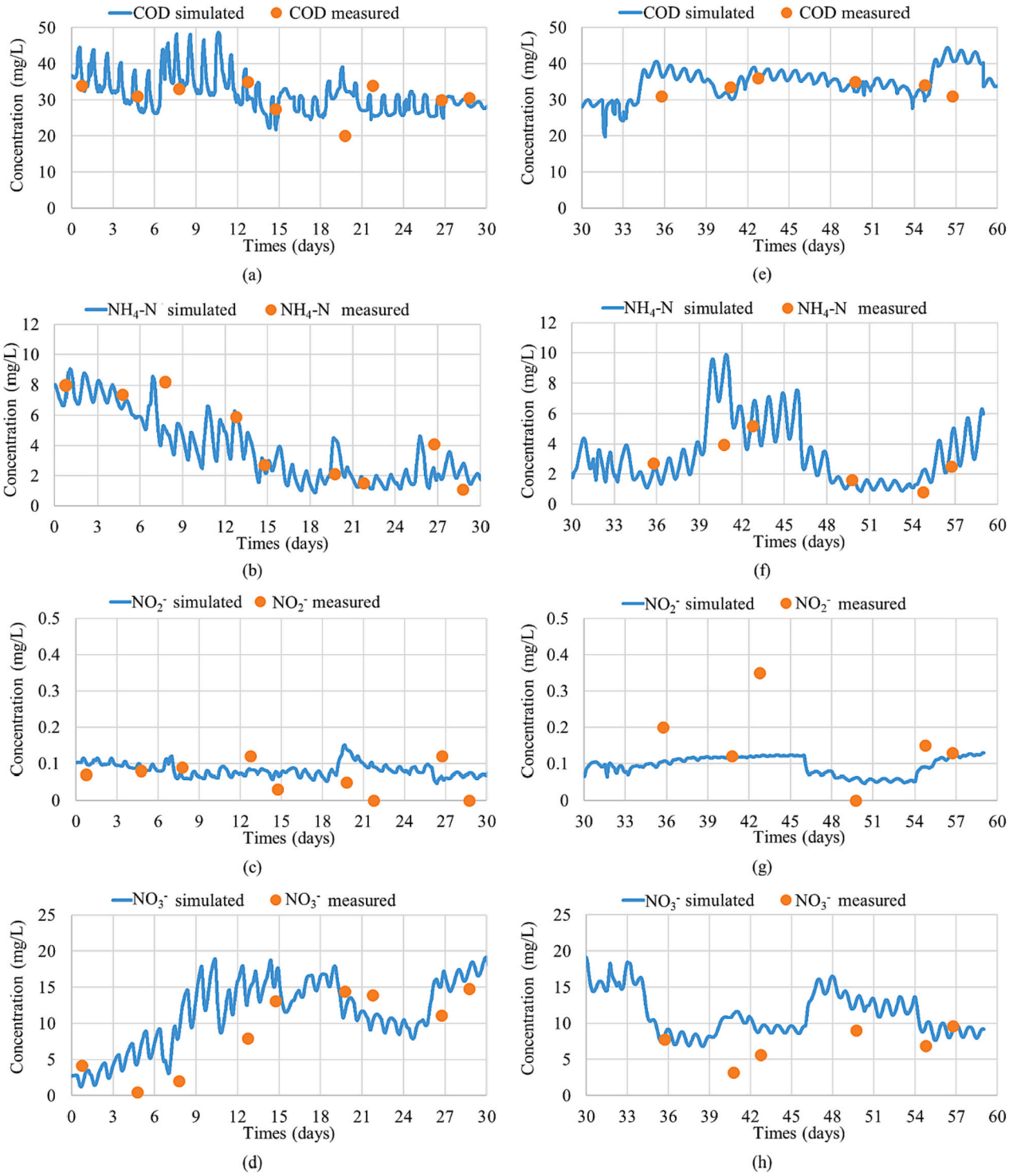

Fig. 5. Results of calibration (a-d) and validation (e-h) of the model.

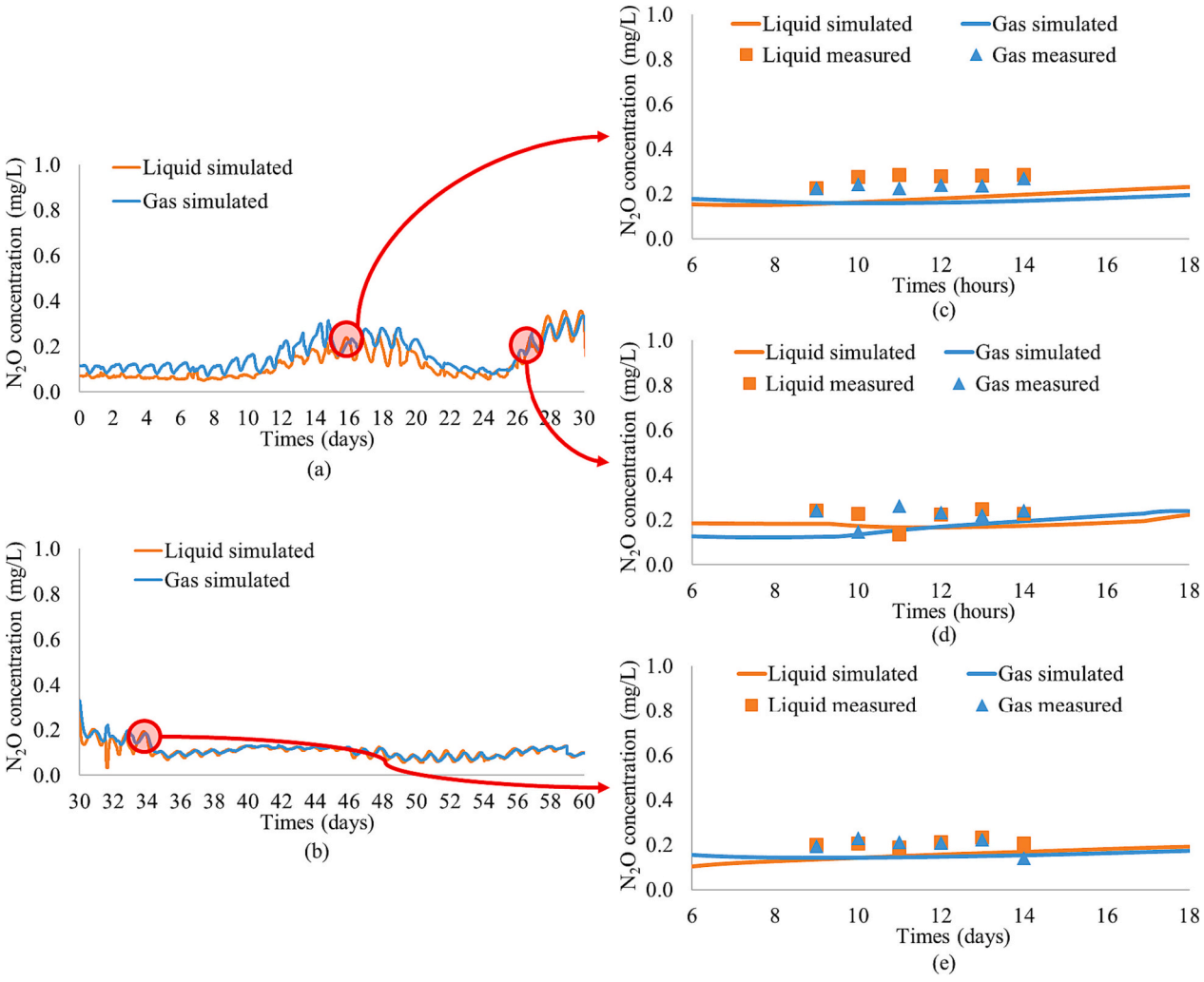

Fig. 6. Simulated N_2O concentrations in liquid and gas for calibration (a) and validation (b) periods in comparison to hourly sampling campaigns 1 (c), 2 (d), and 3 (e).

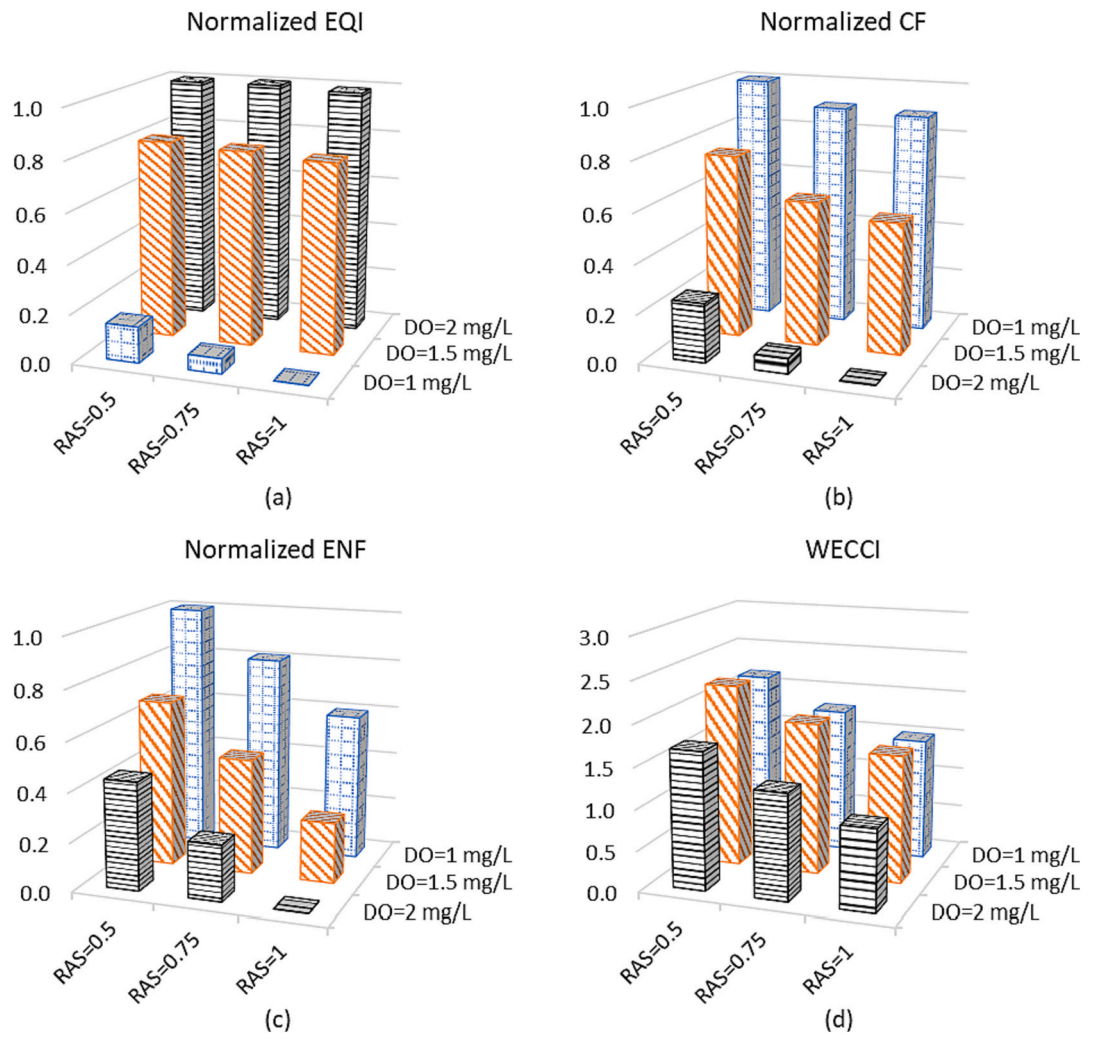

Fig. 7. Comparison of normalised EQI, normalised CF, normalised ENF, and WECII estimated with different RAS ratio and DO concentration

WECCI is the sum of normalised EQI, normalised CF, and normalised ENF (Fig. 7 (d)). The best WECCI was chosen as the optimum scenario when the DO concentration is 1.5 mg/L and the RAS ratio is 0.5 mg/L. On the other hand, the lowest WECCI (the worst scenario) belonged to operational conditions in which the DO concentration is 2 mg/L and the RAS ratio is 1. The WECCI is a measure of the efficiency of WWTPs in terms of effluent quality, energy consumption, and carbon footprint. The scenario analyses revealed that effluent quality and carbon footprint exhibited comparable patterns, but there was a trade-off between these two factors and the energy footprint. It suggests that, efforts to improve effluent quality may coincide with reductions in the carbon footprint. However, improving effluent quality and reducing the carbon footprint objectives can conflict with the goal of minimising energy consumption (Monteiro et al., 2022). Because energy-intensive processes, such as aeration, are necessary to achieve high-effluent quality (Fig. 7 (a)). Therefore, finding the right balance becomes imperative. In addressing this trade-off, technological innovation becomes a key driver. The development and adoption of energy-efficient treatment technologies, advanced process control systems, and renewable energy sources can help WWTPs strike a more favourable balance. Overall, the study emphasised the complexity of optimisation of WWTP and the importance of considering multiple factors. Therefore, to optimise WWTPs, a comprehensive analysis should be conducted, taking into account different aspects. This holistic approach is essential for ensuring that WWTPs meet environmental standards, operate efficiently, and contribute to a sustainable future.

4. Conclusions

ASM1 was modified to model N_2O emissions with a plant-wide modelling approach, and Corleone WWTP (Italy) with aeration and sedimentation units was used as a case study. The major results are summarised below:

- The new ASM1 + N_2O model includes processes related to heterotrophic, ammonia-oxidising, and nitrite-oxidising biomass and N_2O stripping from liquid phase to gas phase.
- The model was calibrated and validated for different sets of 30-day data and hourly sampling data was used to calibrate N_2O in liquid and gas.
- Nine different DO concentration and RAS ratio scenarios were simulated dynamically to compare EQI, CF, and ENF synergistically by WECCI.
- The direct and indirect GHG emissions of Corleone WWTP (related with baseline scenario for which DO = 2 mg/L and RAS = 0.66 were estimated as 0.58 kg CO_2eq/d and 0.27 kg CO_2eq/d, respectively.
- It was found that DO concentration is more effective on EQI and direct emissions than the RAS ratio.
- The best operation scenario was observed at a DO concentration of 1.5 mg/L and RAS ratio of 0.5 for Corleone WWTP; these value differ from the baseline scenario conditions (DO = 2 mg/L and RAS = 0.66).

CRediT authorship contribution statement

Hazal Gulhan: Methodology, software, visualization, validation, writing original draft.

Alida Cosenza: Methodology, software, visualization, validation, writing original draft.

Giorgio Mannina: Conceptualization, supervision, visualization, writing - Review & Editing.

Declaration of competing interest

The authors declare that they have no known competing financial interests or personal relationships that could have appeared to influence the work reported in this paper.

Data availability

The data that has been used is confidential.

Acknowledgement

This work was funded by the project "Achieving wider uptake of water-smart solutions— WIDER UPTAKE" (grant agreement number: 869283) financed by the European Union's Horizon 2020 Research and Innovation Programme, in which the author of this paper, Giorgio Mannina, is the principal investigator for the University of Palermo, Italy. The UNIPA project website can be found at: https://wideruptake.unipa.it/ (accessed on 28 July 2022).

References

Abulimiti, A., Wang, X., Kang, J., Li, L., Wu, D., Li, Z., Piao, Y., Ren, N., 2022. The trade-off between N_2O emission and energy saving through aeration control based on dynamic simulation of full-scale WWTP. Water Res. 223, 118961. https://doi.org/10.1016/j.watres.2022.118961.

Arjen, Y.H., Ashok, K.C., Maite, M.A., Mesfin, M.M., 2012. The Water Footprint Assessment Manual. London, Washington DC.

Blomberg, K., Kosse, P., Mikola, A., Kuokkanen, A., Fred, T., Heinonen, M., Mulas, M., Lübken, M., Wichern, M., Vahala, R., 2018. Development of an extended ASM3 model for predicting the nitrous oxide emissions in a full-scale wastewater treatment plant. Environ. Sci. Technol 52, 5803–5811. https://doi.org/10.1021/acs.est.8b00386.

Caniani, D., Caivano, M., Pascale, R., Bianco, G., Mancini, I.M., Masi, S., Rosso, D., 2019. CO_2 and N_2O from water resource recovery facilities: evaluation of emissions from biological treatment, settling, disinfection, and receiving water body. Sci. Total Environ. 648, 1130–1140. https://doi.org/10.1016/j.scitotenv.2018.08.150.

Cosenza, A., Di Trapani, D., Gulhan, H., Mineo, A., Bosco Mofatto, P.M., Mannina, G., 2023. Reduction of sewage sludge and N2O emissions by an Oxic Settling Anaerobic (OSA) process: the case study of Corleone Wastewater Treatment Plant. Submitted (under review) to Science of The Total Environment.

Copp, J.B. (Ed.), 2002. The COST Simulation Benchmark - Description and Simulator Manual. Office for Official Publications of the European Communities, Luxembourg, ISBN 92-894-1658-0.

Daelman, M.R.J., van Voorthuizen, E.M., van Dongen, L.G.J.M., Volcke, E.I.P., van Loosdrecht, M.C.M., 2013. Methane and nitrous oxide emissions from municipal wastewater treatment – results from a long-term study. Water Sci. Technol. 67 (10), 2350–2355. https://doi.org/10.2166/wst.2013.109.

GWRC, 2011. N_2O and CH_4 Emission from Wastewater Collection and Treatment Systems - Technical Report. London. ISBN 978.90.77622.24.7.

Hauduc, H., Rieger, L., Takács, I., Héduit, A., Vanrolleghem, P.A., Gillot, S., 2010. A systematic approach for model verification: application on seven published activated sludge models. Water Sci. Technol. 61 (4), 825–839. https://doi.org/10.2166/wst.2010.898.

Henze, M., Gujer, W., Mino, T., van Loosdrecht, M.C.M., 2000. Activated Sludge Models: ASM1, ASM2, ASM2d and ASM3. IWA Publishing, London. https://doi.org/10.1007/978-981-10-1866-4.

Hiatt, W.C., Grady, C.P.L., 2008. An updated process model for carbon oxidation, nitrification, and denitrification. Water Environ. Res. 80 (11), 2145–2156. https://doi.org/10.2175/106143008x304776.

IPCC, 2022. Intergovernmental Panel on Climate Change Sixth Assessment Report. https://www.ipcc.ch/report/ar6/wg3/.

Kampschreur, M.J., Temmink, H., Kleerebezem, R., Jetten, M.S., van Loosdrecht, M.C., 2009. Nitrous oxide emission during wastewater treatment. Water Res. 43 (17), 4093–4103. https://doi.org/10.1016/j.watres.2009.03.001.

Kim, S., Miyahara, M., Fushinobu, S., Wakagi, T., Shoun, H., 2010. Nitrous oxide emission from nitrifying activated sludge dependent on denitrification by ammonia-oxidising bacteria. Bioresour. Technol. 101 (11), 3958–3963. https://doi.org/10.1016/j.biortech.2010.01.030.

Law, Y., Lant, P., Yuan, Z., 2011. The effect of pH on N_2O production under aerobic conditions in a partial nitritation system. Water Res. 45 (18), 5934–5944. https://doi.org/10.1016/j.watres.2011.08.055.

Lee, Y.J., Lin, R.I., Lei, Z., 2022. Nitrous oxide emission mitigation from biological wastewater treatment – a review. Bioresour. Technol. 362, 127747.

Lu, X., Pereira, T.D.S., Al-Hazmi, H.E., Majtacz, J., Zhou, Q., Xie, L., Makinia, J., 2018. Model-based evaluation of N2O production pathways in the anammox-enriched granular sludge cultivated in a sequencing batch reactor. Environ. Sci. Technol. 52, 2800–2809. https://doi.org/10.1021/acs.est.7b05611.

Maktabifard, M., Blomberg, K., Zaborowska, E., Mikola, A., Makinia, J., 2022. Model-based identification of the dominant N_2O emission pathway in a full-scale activated sludge system. J. Clean. Prod. 336, 130347.

Mannina, G., Cosenza, A., 2015. Quantifying sensitivity and uncertainty of a new mathematical model for the evaluation of greenhouse gas emissions from membrane bioreactors. J. Membr. Sci. 475, 80–90.

Mannina, G., Cosenza, A., Vanrolleghem, P.A., Viviani, G., 2011. A practical protocol for calibration of nutrient removal wastewater treatment models. J. Hydroinf. 13 (4), 575–595.

Mannina, G., Ekama, G., Caniani, D., Cosenza, A., Esposito, G., Gori, R., Garrido-Baserba, M., Rosso, D., Olsson, G., 2016. Greenhouse gases from wastewater treatment — a review of modelling tools. Sci. Total Environ. 551-552, 254–270. https://doi.org/10.1016/j.scitotenv.2016.01.163.

Mannina, G., Capodici, M., Cosenza, A., Di Trapani, D., Laudicina, V.A., Ødegaard, H., 2017a. Nitrous oxide from moving bed based integrated fixed film activated sludge membrane bioreactors. J. Environ. Manag. 187, 96–102.

Mannina, G., Cosenza, A., Ekama, G.A., 2017b. Greenhouse gases from membrane bioreactors: mathematical modelling, sensitivity and uncertainty analysis. Bioresour. Technol. 239, 353–367.

Mannina, G., Cosenza, A., Viviani, G., Ekama, G.A., 2018. Sensitivity and uncertainty analysis of an integrated ASM2d MBR model for wastewater treatment. Chem. Eng. J. 351, 579–588.

Mannina, G., Rebouças, T.F., Cosenza, A., Chandran, K., 2019. A plant-wide wastewater treatment plant model for carbon and energy footprint: model application and scenario analysis. J. Clean. Prod. 217, 244–256. https://doi.org/10.1016/j.jclepro.2019.01.255.

Mannina, G., Badalucco, L., Barbara, L., Cosenza, A., Di Trapani, D., Gallo, G., Laudicina, V.A., Marino, G., Muscarella, S.M., Presti, D., Helness, H., 2021a. Enhancing a Transition to a Circular Economy in the Water Sector: The EU Project WIDER UPTAKE. Water 13, 946.

Mannina, G., Alduina, R., Badalucco, L., Barbara, L., Capri, F.C., Cosenza, A., Di Trapani, D., Gallo, G., Laudicina, V.A., Muscarella, S.M., Presti, D., 2021b. Water resource recovery facilities (Wrrfs): The case study of Palermo university (Italy). Water 13, 3413.

Mannina, G., Badalucco, L., Barbara, L., Cosenza, A., Di Trapani, D., Laudicina, V.A., Muscarella, S.M., Presti, D., 2022. Roadmapping the Transition to Water Resource Recovery Facilities: The Two Demonstration Case Studies of Corleone and Marineo (Italy). Water 14, 156.

Massara, T.M., Malamis, S., Guisasola, A., Baeza, J.A., Noutsopoulos, C., Katsou, E., 2017. A review on nitrous oxide (N_2O) emissions during biological nutrient removal from municipal wastewater and sludge reject water. Sci. Total Environ. 596-597, 106–123. https://doi.org/10.1016/j.scitotenv.2017.03.191.

Massara, T.M., Solís, B., Guisasola, A., Katsou, E., Baeza, J.A., 2018. Development of an ASM2d-N_2O model to describe nitrous oxide emissions in municipal WWTPs under dynamic conditions. Chem. Eng. J. 335, 185–196. https://doi.org/10.1016/j.cej.2017.10.119.

Monteiro, M.T.T., Santo, I.E., Rodrigues, H.S., 2022. An optimal control problem applied to a wastewater treatment plant. Discrete Contin. Dyn. Syst. - S. 15 (3).

Ni, B.J., Yuan, Z., 2015. Recent advances in mathematical modelling of nitrous oxides emissions from wastewater treatment processes. Water Res. 87, 336–346.

Ni, B.J., Ye, L., Law, Y., Byers, C., Yuan, Z., 2013. Mathematical modeling of nitrous oxide (N2O) emissions from full-scale wastewater treatment plants. Environ. Sci. Technol. 47 (14), 7795–7803.

Ni, X., Huang, X., Guo, R., Wang, J., Peng, K., Zhang, W., Zhu, Y., Yang, W., Wang, L., Cai, C., Liu, J., Liu, E., 2023. Water–energy–carbon synergies and trade-offs: a daily nexus analysis for wastewater treatment plants. Resour. Conserv. Recycl. 188, 106712. https://doi.org/10.1016/j.resconrec.2022.106712.

Rosso, D., Larson, L.E., Stenstrom, M.K., 2008. Aeration of large-scale municipal wastewater treatment plants: state of the art. Water Sci. Technol. 57 (7), 973–978.

Schulthess, R.V., Gujer, W., 1996. Release of nitrous oxide (N_2O) from denitrifying activated sludge: verification and application of a mathematical model. Water Res. 30 (3), 521–530. https://doi.org/10.1016/0043-1354(95)00204-9.

Solís, B., Guisasola, A., Pijuan, M., Corominas, L., Baeza, J.A., 2022. Systematic calibration of N2O emissions from a full-scale WWTP including a tracer test and a global sensitivity approach. Chem. Eng. J. 435, 134733. https://doi.org/10.1016/j.cej.2022.134733.

Thakur, I.S., Medhi, K., 2019. Nitrification and denitrification processes for mitigation of nitrous oxide from waste water treatment plants for biovalorization: challenges and opportunities. Bioresour. Technol. 282, 502–513. https://doi.org/10.1016/j.biortech.2019.03.069.

Vasilaki, V., Massara, T., Stanchev, P., Fatone, F., Katsou, E., 2019. A decade of nitrous oxide (N_2O) monitoring in full-scale wastewater treatment processes: a critical review. Water Res. 161, 392–412. https://doi.org/10.1016/j.watres.2019.04.022.

World Resource Institute, 2014. WRI's Sustainability Data. https://www.wri.org/sustainability-wri/dashboard.

Wunderlin, P., Mohn, J., Joss, A., Emmenegger, L., Siegrist, H., 2012. Mechanisms of N_2O production in biological wastewater treatment under nitrifying and denitrifying conditions. Water Res. 46 (4), 1027–1037. https://doi.org/10.1016/j.watres.2011.11.080.

Zaborowska, E., Lu, X., Makinia, J., 2019. Strategies for mitigating nitrous oxide production and decreasing the carbon footprint of a full-scale combined nitrogen and phosphorus removal activated sludge system. Water Res. 162, 53–63. https://doi.org/10.1016/j.watres.2019.06.057.